Procollagen Lysyl Hydroxylase 2 is Essential for Hypoxia-Induced Breast Cancer Metastasis

Daniele Gilkes,[1,2,4] Saumendra Bajpai,[4,5] Carmen Chak-Lui Wong,[1,2] Pallavi Chaturvedi,[1,2] Maimon E. Hubbi,[1,2] Denis Wirtz,[4,5] and Gregg L. Semenza[1,2,3,4*]

[1]Vascular Program, Institute for Cell Engineering
[2]McKusick-Nathans Institute of Genetic Medicine
[3]Departments of Pediatrics, Oncology, Medicine, Radiation Oncology, and Biological Chemistry
Johns Hopkins University School of Medicine Baltimore, MD 21205, USA

[4]Johns Hopkins Physical Sciences - Oncology Center
[5]Department of Chemical and Biomolecular Engineering
Johns Hopkins University, Baltimore, MD 21218, USA

***Correspondence:** Email: gsemenza@jhmi.edu; Fax: 443-287-5618

Running Title: PLOD2 is essential for hypoxia-induced metastasis

Keywords: lysyl hydroxylase, PLOD2, hypoxia, HIF-1, collagen

Abstract

Metastasis is the leading cause of death among patients who have breast cancer. Understanding the role of the extracellular matrix in the metastatic process may lead to the development of improved therapies to treat cancer patients. Intratumoral hypoxia, found in the majority of breast cancers, is associated with an increased risk of metastasis and mortality. We found that in hypoxic breast cancer cells, HIF-1 activates transcription of the *PLOD1* and *PLOD2* genes encoding procollagen lysyl hydroxylases that are required for the biogenesis of collagen, which is a major constituent of the extracellular matrix. High *PLOD2* expression in breast cancer biopsies is associated with increased risk of mortality. We demonstrate that PLOD2 is critical for fibrillar collagen formation by breast cancer cells, increases tumor stiffness, and is required for metastasis to lymph nodes and lungs.

Introduction

During breast cancer progression, increased cancer cell proliferation and oxygen consumption lead to significantly reduced oxygen availability as compared to normal breast tissue (1, 2). Intratumoral hypoxia is associated with increased risk of invasion, metastasis, treatment failure, and patient mortality (3). The ability of cancer cells to survive and adapt to hypoxia depends on hypoxia-inducible factor 1 (HIF-1) and HIF-2, which induce the expression of more than 1000 target genes, many of which are involved in angiogenesis, glucose utilization, cell proliferation, invasion, and metastasis (4). HIF-1 is a heterodimeric protein that is composed of an O_2-regulated HIF-1α subunit and a constitutively expressed HIF-1β subunit (5). In mouse models, decreasing HIF-1α expression impedes tumor growth, angiogenesis, and breast cancer metastasis (6-10). In human breast cancer biopsies, increased HIF-1α protein levels are associated with an increased risk of metastasis and mortality, which is independent of patient stage, estrogen receptor expression, or lymph node status (11-15). HIF-2α is also O_2 regulated, dimerizes with HIF-1β, and promotes breast cancer progression (16).

Mammographic breast tissue density is a risk factor for breast cancer and collagen is a major contributor to tissue density (17-19). Fibrotic breast cancers have the poorest prognosis and highest rate of recurrence (20). During breast cancer progression, collagen fibers increase in density, straighten, bundle, and align (21). Several groups have observed that tumor cells preferentially invade along aligned collagen fibers (21-23). Furthermore, the pattern and extent of collagen alignment has prognostic significance in breast cancer (24). Increases in collagen crosslinking promote extracellular matrix (ECM) stiffening, which enhances cell growth, survival, tension, integrin signaling and focal adhesion formation (25-27).

Collagens are the major fibrous proteins in the ECM and the most abundant proteins in the human body, modulating cell behavior primarily through interactions with integrins. Collagen biogenesis is a complex process involving extensive post-translational modifications, including lysine hydroxylation (28). Hydroxylation of procollagen lysine residues occurs intracellularly and generates specific sites for glycosylation (29). Once collagen is secreted, collagen crosslinking occurs on lysine and hydroxylysine residues by the extracellular enzyme lysyl oxidase (30). Cross-links involving hydroxylysine residues are more stable than those derived from lysine residues and less susceptible to matrix metalloproteinase degradation (31, 32). Thus, lysyl hydroxylases and oxidases are the key mediators of collagen cross-linking.

Three lysyl hydroxylase genes (*PLOD1*, *PLOD2*, and *PLOD3*) encoding isoforms of procollagen-lysine, 2-oxyglutarate, 5-dioxygenase have been characterized (33). PLOD2 specifically hydroxylates lysines in the telopeptide of procollagens, whereas PLOD1 is responsible for lysine hydroxylation in the α-helical or central domain; the substrate specificity of PLOD3 is unknown (34-37). Enzymatic collagen cross-linking by lysyl oxidases occurs by the specific oxidative deamination of telopeptide lysine or hydroxylysine residues (30). Telopeptide lysines form crosslinks which are commonly found in soft tissue such as the skin (38). Telopeptide hydroxylysine residues react to form crosslinks found in stiffer tissue such as cartilage and bone. Accordingly, overaccumulation of collagen in fibrotic conditions is caused by overhydroxylation of the collagen telopeptides and an increased amount of pyridinoline cross-links formed by hydroxylated telopeptide lysines (39-41). Pyridinoline crosslinks are more stable and resistant to degradation. Furthermore, PLOD2 is the only lysyl hydroxylase that causes changes to collagen cross-linking patterns (41). Interestingly, while PLOD2-deficiency leads to

embryonic lethality in mice, PLOD1-deficeint mice have an normal life span suggesting that PLOD2 may compensate for losses in PLOD1 expression (42). Although the role of PLODs in cancer has not been determined, their significance is evident in other diseases. Lysine hydroxylation is impaired in Bruck Syndrome (36) and Ehlers-Danlos Syndrome Type VIA (43), whereas it is increased in fibrotic diseases (39).

We have previously demonstrated that inhibition of HIF activity in breast cancer cells by RNA interference or treatment with digoxin, a drug that blocks HIF-1α protein expression, decreases both primary tumor growth and metastasis to lungs and lymph nodes (9, 10, 44, 45). Several studies have shown the importance of hypoxia-induced and HIF-regulated expression of LOX, LOX-like 2 (LOXL2), and LOXL4 for metastasis (10, 27, 45-47). Since lysyl hydroxylases are an integral part of collagen crosslinking and act upstream of LOX, we investigated their role in breast cancer metastasis. We analyzed the role of HIFs in regulating PLOD1 and PLOD2 expression in hypoxic breast cancer cells and investigated the effects of hypoxia-induced PLOD2 expression on tumor ECM properties and breast cancer metastasis.

Materials and Methods

Cell lines and culture

MDA-MB-231 (48) and MDA-MB-435 (49) human breast cancer cells were obtained from the NCI PS-OC Network Bioresource Core Facility and maintained in DMEM containing 10% fetal bovine serum (FBS) and antibiotics at 37°C in a 5% CO_2, 95% air incubator (20% O_2). The cells tested negative for the presence of mycoplasma according to procedures utilized by the

Johns Hopkins fragment analysis core using a PCR based detection kit. The cell lines were authenticated by short tandem repeat profiling. Hypoxic cells (1% O_2) were maintained at 37°C in a modular incubator chamber (Billups-Rothenberg) flushed with a gas mixture containing 1% O_2, 5% CO_2, and 94% N_2. HIF-1α-null mouse embryo fibroblasts were described previously (50).

shRNA, lentiviruses, and transduction

Vectors encoding short hairpin RNA (shRNA) targeting HIF-1α or HIF-2α were previously described (9). pLKO.1-puro shRNA expression vectors targeting PLOD2 were purchased from Sigma-Aldrich. Lentiviruses were packaged in 293T cells by co-transfection with plasmid pCMV-dR8.91 and a plasmid encoding vesicular stomatitis virus G protein, using Lipofectamine 2000 (Invitrogen). Culture supernatants containing the viral particles were collected 48 hours after transfection and filtered using a 0.45-μm membrane. MDA-MB-231 and MDA-MB-435 cells were transduced with viral supernatant supplemented with 8 μg/mL Polybrene (Sigma-Aldrich) and selected in media containing 0.6 μg/mL puromycin.

Immunoblot assays

Aliquots of whole cell lysates prepared in NP-40 buffer (150 mM NaCl, 1% NP-40, 50 mM Tris-HCl, pH 8.0) were fractionated by 8% SDS-PAGE. Conditioned medium was collected from cells and concentrated with 30% ammonium sulfate overnight at 4◦C followed by centrifugation at 30,000 x *g* for 1 hour. Antibodies against HIF-1α (BD Transduction Laboratory), PLOD1, PLOD2, HIF-2α, COL1A1 (Novus Biologicals), and β-actin (Santa Cruz) were used.

Orthotopic implantation and metastasis assays

Studies using 7-10 week-old female NOD-SCID mice (NCI) were approved by the Johns Hopkins University Animal Care and Use Committee and were in accordance with the NIH Guide for the Care and Use of Laboratory Animals. Mammary fat pad (MFP) injection, tumor growth measurements, and human genomic DNA extraction from mouse lungs were previously described (9).

Real-time reverse transcription quantitative PCR (RT-qPCR)

RNA extraction and cDNA synthesis were performed as previously described (9). The fold change in expression of each target mRNA relative to 18S rRNA was calculated based on the threshold cycle (C_t) as $2^{-\Delta(\Delta Ct)}$, where $\Delta C_t = C_t\,(\text{target}) - C_t\,(18S)$ and $\Delta(\Delta C_t) = \Delta C_t\,(20\%\ O_2) - \Delta C_t\,(1\%\ O_2)$.

Fibrillar collagen staining

Tumor sections were stained with 0.1% picrosirius red (Direct Red 80, Sigma) and counterstained with Weigert's hematoxylin. To reveal fibrillar collagen, stained sections were imaged with an Olympus IX51 fluorescence microscope fitted with an analyzer (U-ANT) and polarizer (U-POT). The percent fibrillar collagen was quantified by calculating the area of staining (by thresholding) relative to the total area of the section using MetaMorph analysis software.

Tumor collagen content measurements

Cells were harvested and hydrolyzed in 6N HCl for 16 hours at 116^{o}C overnight. Tumor tissue was excised, dried in a vacuum, and weighed followed by hydrolysis in 6N HCl for 16 hours at 116^{o}C. Hydroxyproline content was determined by a colorimetric method (51). Total protein was measured by the Bradford assay using a commercial kit (BioRad).

Immunohistochemistry

Tumors, lungs, and lymph nodes were fixed in 10% formalin and paraffin embedded. Sections were dewaxed and hydrated. LSAB+ System (DAKO) was used for PLOD2, HIF-1α and vimentin staining according to the manufacturer's instructions. Inflated lung sections were stained with hematoxylin and eosin to detect metastatic foci as previously described (9, 10). DAB and hematoxylin were deconvoluted using Image J and pseudocolored to assess colocalization.

Statistical analysis of microarray data

Gene expression from the Richardson et al. breast cancer data set (52) retrieved from the Oncomine database (http://www.oncomine.org) was analyzed as previously described (53). Unpaired Student's t tests were performed to compare *PLOD1* and *PLOD2* levels in normal versus breast cancer tissue using GraphPad Prism software. The breast invasive carcinoma dataset (54), which included gene expression (expressed as a z-score) and clinical stage, was obtained from The Cancer Genome Atlas (http://tcga-data.nci.nih.gov/tcga/tcgaHome2.jsp). Prognostic significance of PLOD expression in breast cancer patients was examined in the

Pawitan microarray dataset (55). Survival plots and hazard ratio were created using Kaplan-Meier methods in GraphPad Prism Software.

Tumor stiffness measurements

A stepper motor (Harvard Apparatus) was used to impinge a 1-mm diameter probe perpendicular to a freshly excised and immobilized tumor, with the corresponding force measured using a FlexiForce Load/Force Sensor (Tekscan). A constant impingement rate was maintained and force was recorded at 300 Hz using ELF software (TekScan). The slope of the indentation depth (mm) vs impingement force (mN) was used as an effective stiffness measurement. Stiffness values corresponding to the tail of the distribution of slopes were discarded in order to avoid analyzing necrotic regions. For each tumor, 5-6 random locations were probed and mean values were calculated.

Results

PLOD1 and PLOD2 expression is HIF-1-dependent in hypoxic breast cancer cells

The expression of mRNAs encoding PLOD1 and PLOD2 is known to be induced by hypoxia in mouse fibroblast cells (56). To determine if hypoxia induces the expression of procollagen lysyl hydroxylases in human breast cancer cells, we analyzed PLOD1, PLOD2, and PLOD3 mRNA levels in MDA-MB-231 cells following exposure to 20% or 1% O_2 for 24 hours. Expression of PLOD2 mRNA was induced greater than four-fold by hypoxia, whereas PLOD1 mRNA expression was more modestly induced (approximately two-fold), and PLOD3 mRNA expression was not induced by hypoxia. To determine if HIF-1α or HIF-2α was required for

PLOD expression under hypoxic conditions, we generated MDA-MB-231 subclones that were stably transfected with an empty vector (shEV) or expression vector(s) encoding a short hairpin RNA (shRNA) targeted against HIF-1α (sh1α), HIF-2α (sh2α), or HIF-1α and HIF-2α (sh1/2α). Hypoxic induction of PLOD1 and PLOD2 mRNA (Fig. 1A) and protein (Fig. 1B) was blocked when expression of HIF-1α (but not HIF-2α) was abrogated by shRNA. PLOD1 and PLOD2 protein levels were increased within 12 hours and remained elevated for 72 hours of continuous hypoxia (Fig. 1C). Additionally, MDA-MB-231 cells were treated with digoxin, which inhibits HIF-1α protein expression (57). Hypoxia-induced PLOD1 and PLOD2 mRNA expression was significantly decreased in digoxin-treated MDA-MB-231 cells (Fig. 1D). Hypoxia also induced PLOD1 and PLOD2 mRNA expression in wild type, but not in HIF-1α-null, mouse embryo fibroblasts (MEFs) (Fig. S1A).

PLOD expression is associated with human breast cancer progression

To investigate whether procollagen lysyl hydroxylase expression has clinical significance in breast cancer, we compared *PLOD1* and *PLOD2* gene expression in normal human breast and breast cancer tissue using the Oncomine database (www.oncomine.org). Analysis of a representative data set (52) revealed that PLOD1 and especially PLOD2 mRNA expression levels were significantly greater in breast cancer tissue than in normal breast tissue (Fig. 2A). The results were similar when we interrogated the Cancer Genome Atlas (http://tcga-data.nci.nih.gov) for *PLOD1* and *PLOD2* expression in breast cancer versus adjacent normal tissue (Fig. 2B). Kaplan-Meier curves of disease-specific survival stratified by PLOD1 or PLOD2 mRNA levels in a 159-breast cancer patient data set (55) revealed that high PLOD2

expression (greater than the median value) was significantly associated with decreased disease-specific survival (Fig. 2C). Comparing patients whose tumors expressed both PLOD1 and PLOD2 mRNA at greater than median levels with patients whose expression levels were less than the median did not improve the survival prediction. These data indicate that *PLOD2* expression is specifically prognostic in breast cancer.

Decreased PLOD2 expression in breast cancer cells inhibits their invasiveness

Since PLOD2 is the only PLOD family member that is significantly upregulated in fibrosis (36) and *PLOD2* expression was informative for breast cancer patient prognosis, we investigated the role of PLOD2 in breast cancer invasion and metastasis. We generated MDA-MB-231 subclones that were stably transfected with an empty vector (shLKO.1) or a vector encoding either of two different shRNAs against PLOD2 (shPL2-1 and shPL2-2). Immunoblot assays confirmed loss of PLOD2 protein expression in MDA-MB-231 cells (Fig. 3A). The proliferation of subclones transfected with shLKO.1, shPL2-1, or shPL2-2 was similar in tissue culture (Fig. 3B). When injected into the mammary fat pad (MFP) of NOD-SCID mice, the growth rate (Fig. 3C) and final tumor weight (Fig. 3D) were similar among subclones. We confirmed that PLOD2 knockdown was maintained throughout the experiment (Fig. 3E). Immunohistochemical staining of control and knockdown tumors revealed intense PLOD2 staining in perinecrotic (hypoxic) regions of the control shLKO.1 tumors, which was markedly reduced in PLOD2-knockdown tumors (Fig. 3F). HIF-1α and PLOD2 staining co-localized within the perinecrotic region of control tumors (Fig. 3G). Control tumors showed extensive evidence of invasion into adjacent fat and muscle tissue whereas PLOD2-knockdown tumors maintained a distinct tumor-stroma

boundary (Fig. 3H). Taken together, these data show that *PLOD2* expression does not affect tumor growth but promotes local tissue invasion.

Decreased PLOD2 expression in breast cancer cells inhibits metastasis

Primary tumors derived from the injection of MDA-MB-231 cells into the MFP of NOD-SCID mice spontaneously metastasize to the lungs. The overall metastatic burden in the lungs was quantified by isolating genomic DNA from the mouse lung followed by quantitative real-time PCR (qPCR) using primers that only amplify human DNA (Fig. 4A). Lung metastasis was also assessed histologically by hematoxylin and eosin staining (Fig. 4B). The percentage of the lung occupied by breast cancer cells (Fig. 4C) and the number of foci in each section (Fig. 4D) confirmed the qPCR results (Fig. 4A).

We also assessed breast cancer cell infiltration of the ipsilateral axillary LNs in control and PLOD2-knockdown tumor-bearing mice by immunohistochemical staining of human vimentin. The lymph nodes of mice that received MFP injection of shLKO.1 control cells were enlarged and completely infiltrated with breast cancer cells, whereas the follicular lymph node structure and size were maintained in the PLOD2-knockdown tumor-bearing mice (Fig. 4E). Using imaging software, quantitative analysis of lymph nodes was performed by separating the staining signals into a vimentin signal (Fig. 4F, left) and a hematoxylin signal (Fig. 4F, center). The area of vimentin staining within the lymph node was thresholded (Fig. 4F, right) and quantified (Fig. 4G). Lymph node infiltration by PLOD2-deficient breast cancer cells was reduced by greater than 4-fold (Fig. 4G). Taken together, the data presented in Fig. 4 demonstrate that PLOD2 expression is essential for breast cancer metastasis to lung and lymph nodes.

PLOD2 knockdown prevents fibrillar collagen formation in breast tumors

To determine if PLOD2 knockdown inhibits collagen secretion, we analyzed the levels of collagen 1A1 in conditioned media from MDA-MB-231 subclones following 72 hours of culture. Collagen secretion by MDA-MB-231 cells was not affected by PLOD2 knockdown (Fig. 5A). We utilized the Erhlich method (58) to assess overall collagen content in control and PLOD2-knockdown tumors. The procedure involves the hydrolysis of tumor tissue and subsequent determination of hydroxyproline content. Given that ~12.5% of collagen consists of hydroxyproline, the amount of collagen in the tissue can be readily determined. Using this method, we determined that the overall collagen content in primary tumors was 8% of the total protein. PLOD2-knockdown did not affect overall collagen deposition in tumors (Fig. 5B). Since PLOD2 is important for collagen crosslinking, which is required for the formation of collagen fibers, we next analyzed fibrillar collagen content in control and PLOD2- knockdown tumor sections, using picrosirius red staining. Crosslinked collagen fibrils stained with picrosirius red can be detected when viewed under circularly polarized light. Collagen fibers were concentrated and aligned in the perinecrotic (hypoxic) regions of control tumors and absent in PLOD2-deficient tumors (Fig. 5C). Using image analysis to threshold the collagen fibers and compare the area occupied by collagen fibers with the total area of tumor in the section revealed a greater than 50% reduction in collagen fiber formation (Fig. 5D), which was associated with a corresponding decrease in tumor stiffness (Fig. 5E), in PLOD2-deficient tumors. Staining of serial sections revealed co-localization of fibrillar collagen (picrosirius red staining) and PLOD2 (immunohistochemistry) in perinecrotic regions (Fig. 5F), which is consistent with the biochemical function of PLOD2 in promoting fibrillar collagen formation. Taken together, the

results shown in Fig. 5 demonstrate that PLOD2 does not affect collagen deposition but is required for collagen fibers to form within tumors.

PLOD2 activity is required for metastasis of MDA-MB-435 breast cancer cells

The results presented in Fig. 1-5 demonstrate a critical role for PLOD2 expression in local tissue invasion and metastasis of MDA-MB-231 cells to the axillary lymph node and lungs without affecting primary tumor growth. To demonstrate that these effects of PLOD2 are a general feature of metastatic breast cancer cells, we utilized MDA-MB-435 cells (49). We generated MDA-MB-435 subclones stably transfected with an empty vector (shLKO.1) or a vector expressing either of two shRNAs against PLOD2 (shPL2-1 or shPL2-2) (Fig. 6A, Fig. S2) and orthotopically injected them into the MFP of NOD-SCID mice. Primary tumor growth was unaffected by the knockdown of PLOD2 (Fig. 6B), whereas local invasion of breast cancer cells was evident in control tumors only (Fig. 6C). Lung metastasis was significantly impaired by PLOD2 knockdown (Fig. 6D-G). Human vimentin staining of mouse lymph nodes (Fig. 6H) revealed an 80% reduction in lymph node infiltration by PLOD2-deficient breast tumors (Fig. 6I). Finally, decreasing PLOD2 in MDA-MB-435 cells reduced tumor stiffness (Fig. 6J). Taken together, the results presented in Fig. 1-6 demonstrate that hypoxia induces PLOD2 expression in two different metastatic breast cancer cell lines with similar effects on tumor stiffness, local invasion, and metastasis to lungs and lymph nodes.

Discussion

HIF-1 regulates multiple steps in collagen biogenesis

Multiple sequential steps are required for collagen fibril formation including synthesis of procollagen polypeptides, hydroxylation of proline and lysine residues, triple helix formation, glycosylation, secretion to the extracellular space, cleavage of propeptides, deposition, and cross linking of collagen molecules (fiber formation). Several studies have highlighted the role of hypoxia and HIF-1 in inducing the expression of multiple members of the LOX family of enzymes, which crosslink collagen that has been secreted into the ECM and promote breast cancer metastasis (45, 46). The present study demonstrates that HIF-1 also promotes the initiating step of collagen crosslinking, which involves hydroxylation of collagen lysine residues, by activating *PLOD1* and *PLOD2* gene expression in hypoxic breast cancer cells (Fig. 7).

Collagen crosslinking is sufficient to promote metastasis

Recent evidence shows that LOX induces increased breast cancer stiffness by promoting collagen crosslinking, which facilitates integrin clustering to reduce tumor latency (27). Tumor-secreted LOX also has effects on collagen crosslinking in the lungs, which promotes pre-metastatic niche formation (47). Since LOX affects ECM both in the primary tumor and at the metastatic site, it is difficult to discern whether increased collagen crosslinking in the tumor itself or within the lung parenchyma is necessary to promote metastasis. In contrast, PLOD2 is an intracellular enzyme that only promotes metastasis by cross-linking within the primary tumor. Our results demonstrate that inhibition of PLOD2 expression prevents collagen fiber formation in tumors and provides the first evidence that alterations in the fibrillar structure of collagen

caused by changes in crosslinking specifically within a primary breast tumor promotes lung and lymph node metastasis. Importantly, addition of exogenous fibrillar collagen, but not denatured collagen, was sufficient to increase metastasis.

The role of PLOD2 in establishing a tumor ECM that facilitates metastasis

PLOD2 likely influences metastasis by several mechanisms. First, fibrillar collagen content affects the biophysical properties of the ECM, thereby promoting invasion (27). In our study, PLOD2 knockdown reduced overall tumor stiffness and fibrillar collagen formation without affecting collagen deposition, leading to impaired local invasion into the surrounding tissue and decreased lymphatic and hematogenous metastasis to axillary lymph nodes and lungs, respectively. Second, collagen fiber alignment directs the motility of cancer cells *in vivo* (22). We found aligned collagen fibers were localized to perinecrotic (hypoxic) regions of tumors where the highest levels of PLOD2 expression were detected. Third, tissue fibrosis influences tumor progression by regulating soluble growth factor availability, distribution, and presentation to cells (59).

PLOD2 expression and breast cancer prognosis

We found that high levels of PLOD2 mRNA in the primary tumor are significantly associated with increased risk of mortality in women with breast cancer. Although prior to our work PLOD2 had not been studied intensively in the context of tumor biology, a survey of the literature suggests that it may be relevant for cancer prognosis. In several microarray studies, *PLOD2* was identified in gene signatures associated with cervical cancer, glioblastoma, hepatocellular carcinoma and gastric cancer (60-63). Furthermore, *PLOD2* was one of 17 genes

implicated as a potential mediator of breast cancer metastasis to the brain (64). Interestingly, in agreement with the results of our study, neither PLOD1 nor PLOD3 was implicated in these studies. These data indicate that our findings in a mouse model of breast cancer are likely to have clinical significance.

PLOD2 and breast cancer treatment

Fibrotic breast cancers have the poorest prognosis and highest rate of recurrence (20). An evaluation of tumor biopsies from 196 breast cancer patients identified a histological signature characterized by bundles of straightened and aligned collagen fibers that predicted adverse patient outcome, which was independent of tumor grade or size, estrogen or progesterone receptor status, $HER2^{neu}$ status, lymph node status, or tumor subtype (24). This finding, taken together with the dramatic effect of PLOD2 knockdown on fibrillar collagen formation, indicates that procollagen lysyl hydroxylases represent a potential therapeutic target for the prevention of breast cancer metastasis. Drugs such as digoxin that inhibit HIF-1 activity may be beneficial because they reduce tumor fibrosis by blocking multiple steps in collagen biogenesis (Fig. 7) as well as impairing other critical steps in the metastatic process (9, 10, 44, 45). Furthermore, specific inhibitors of HIF-1 or procollagen lysyl hydroxylase activity may block collagen fiber biogenesis by both cancer cells and cancer-associated fibroblasts and their use can be guided by the analysis of HIF-1α or PLOD2 expression in diagnostic cancer biopsies.

Acknowledgments

We are grateful to Karen Padgett of Novus Biologicals for generous gifts of antibodies against PLOD1, PLOD2, HIF-2α, and COL1A1. This work was supported in part by National Cancer Institute grant U54-CA143868. G.L.S. is the C. Michael Armstrong Professor at the Johns Hopkins University School of Medicine and an American Cancer Society Research Professor. D.M.G is the recipient of a Susan G. Komen Breast Cancer Foundation Post-Doctoral Fellowship Award.

References

1. Dewhirst MW. Intermittent hypoxia furthers the rationale for hypoxia-inducible factor-1 targeting. Cancer Res 2007;67:854-5.
2. Brahimi-Horn MC, Chiche J, Pouyssegur J. Hypoxia and cancer. J Mol Med 2007;85:1301-7.
3. Gillies RJ, Gatenby RA. Hypoxia and adaptive landscapes in the evolution of carcinogenesis. Cancer Metastasis Rev 2007;26:311-7.
4. Semenza GL. Defining the role of hypoxia-inducible factor 1 in cancer biology and therapeutics. Oncogene 2010;29:625-34.
5. Wang GL, Jiang BH, Rue EA, Semenza GL. Hypoxia-inducible factor 1 is a basic-helix-loop-helix-PAS heterodimer regulated by cellular O2 tension. Proc Natl Acad Sci U S A 1995;92:5510-4.
6. Hiraga T, Kizaka-Kondoh S, Hirota K, Hiraoka M, Yoneda T. Hypoxia and hypoxia-inducible factor-1 expression enhance osteolytic bone metastases of breast cancer. Cancer Res 2007;67:4157-63.
7. Li L, Lin X, Staver M, Shoemaker A, Semizarov D, Fesik SW, et al. Evaluating hypoxia-inducible factor-1α as a cancer therapeutic target via inducible RNA interference in vivo. Cancer Res 2005;65:7249-58.
8. Liao D, Corle C, Seagroves TN, Johnson RS. Hypoxia-inducible factor-1α is a key regulator of metastasis in a transgenic model of cancer initiation and progression. Cancer Res 2007;67:563-72.
9. Zhang H, Wong CC, Wei H, Gilkes DM, Korangath P, Chaturvedi P, et al. HIF-1-dependent expression of angiopoietin-like 4 and L1CAM mediates vascular metastasis of hypoxic breast cancer cells to the lungs. Oncogene 2012;31:1757-70.
10. Wong CC, Gilkes DM, Zhang H, Chen J, Wei H, Chaturvedi P, et al. Hypoxia-inducible factor 1 is a master regulator of breast cancer metastatic niche formation. Proc Natl Acad Sci U S A 2011;108:16369-74.
11. Bos R, van der Groep P, Greijer AE, Shvarts A, Meijer S, Pinedo HM, et al. Levels of hypoxia-inducible factor-1α independently predict prognosis in patients with lymph node negative breast carcinoma. Cancer 2003;97:1573-81.
12. Schindl M, Schoppmann SF, Samonigg H, Hausmaninger H, Kwasny W, Gnant M, et al. Overexpression of hypoxia-inducible factor 1α is associated with an unfavorable prognosis in lymph node-positive breast cancer. Clin Cancer Res 2002;8:1831-7.
13. Generali D, Berruti A, Brizzi MP, Campo L, Bonardi S, Wigfield S, et al. Hypoxia-inducible factor-1α expression predicts a poor response to primary chemoendocrine therapy and disease-free survival in primary human breast cancer. Clin Cancer Res 2006;12:4562-8.
14. Yamamoto Y, Ibusuki M, Okumura Y, Kawasoe T, Kai K, Iyama K, et al. Hypoxia-inducible factor 1α is closely linked to an aggressive phenotype in breast cancer. Breast Cancer Res Treat 2008;110:465-75.

15. Dales JP, Garcia S, Meunier-Carpentier S, Andrac-Meyer L, Haddad O, Lavaut MN, et al. Overexpression of hypoxia-inducible factor HIF-1α predicts early relapse in breast cancer: retrospective study in a series of 745 patients. Int J Cancer 2005;116:734-9.
16. Helczynska K, Larsson AM, Holmquist Mengelbier L, Bridges E, Fredlund E, Borgquist S, et al. Hypoxia-inducible factor-2α correlates to distant recurrence and poor outcome in invasive breast cancer. Cancer Res 2008;68:9212-20.
17. Ramaswamy S, Ross KN, Lander ES, Golub TR. A molecular signature of metastasis in primary solid tumors. Nat Genet 2003;33:49-54.
18. Martin LJ, Boyd NF. Mammographic density. Potential mechanisms of breast cancer risk associated with mammographic density: hypotheses based on epidemiological evidence. Breast Cancer Res 2008;10:201.
19. Provenzano PP, Inman DR, Eliceiri KW, Knittel JG, Yan L, Rueden CT, et al. Collagen density promotes mammary tumor initiation and progression. BMC Med 2008;6:11.
20. Hasebe T, Tsuda H, Tsubono Y, Imoto S, Mukai K. Fibrotic focus in invasive ductal carcinoma of the breast: a histopathological prognostic parameter for tumor recurrence and tumor death within three years after the initial operation. Jpn J Cancer Res 1997;88:590-9.
21. Provenzano PP, Eliceiri KW, Campbell JM, Inman DR, White JG, Keely PJ. Collagen reorganization at the tumor-stromal interface facilitates local invasion. BMC Med 2006;4:38.
22. Wyckoff JB, Wang Y, Lin EY, Li JF, Goswami S, Stanley ER, et al. Direct visualization of macrophage-assisted tumor cell intravasation in mammary tumors. Cancer Res 2007;67:2649-56.
23. Wang W, Wyckoff JB, Frohlich VC, Oleynikov Y, Huttelmaier S, Zavadil J, et al. Single cell behavior in metastatic primary mammary tumors correlated with gene expression patterns revealed by molecular profiling. Cancer Res 2002;62:6278-88.
24. Conklin MW, Eickhoff JC, Riching KM, Pehlke CA, Eliceiri KW, Provenzano PP, et al. Aligned collagen is a prognostic signature for survival in human breast carcinoma. Am J Pathol 2011;178:1221-32.
25. Paszek MJ, Zahir N, Johnson KR, Lakins JN, Rozenberg GI, Gefen A, et al. Tensional homeostasis and the malignant phenotype. Cancer Cell 2005;8:241-54.
26. Lopez JI, Mouw JK, Weaver VM. Biomechanical regulation of cell orientation and fate. Oncogene 2008;27:6981-93.
27. Levental KR, Yu H, Kass L, Lakins JN, Egeblad M, Erler JT, et al. Matrix crosslinking forces tumor progression by enhancing integrin signaling. Cell 2009;139:891-906.
28. Myllyharju J, Kivirikko KI. Collagens, modifying enzymes and their mutations in humans, flies and worms. Trends Genet 2004;20:33-43.
29. Kivirikko KI. Collagen biosynthesis: a mini-review cluster. Matrix Biol 1998;16:355-6.
30. Knott L, Bailey AJ. Collagen cross-links in mineralizing tissues: a review of their chemistry, function, and clinical relevance. Bone 1998;22:181-7.
31. Prockop DJ, Kivirikko KI. Heritable diseases of collagen. N Engl J Med 1984;311:376-86.

32. van der Slot AJ, van Dura EA, de Wit EC, De Groot J, Huizinga TW, Bank RA, et al. Elevated formation of pyridinoline cross-links by profibrotic cytokines is associated with enhanced lysyl hydroxylase 2b levels. Biochim Biophys Acta 2005;1741:95-102.
33. Valtavaara M, Szpirer C, Szpirer J, Myllyla R. Primary structure, tissue distribution, and chromosomal localization of a novel isoform of lysyl hydroxylase (lysyl hydroxylase 3). J Biol Chem 1998;273:12881-6.
34. Steinmann B, Raghunath M. Delayed helix formation of mutant collagen. Science 1995;267:258.
35. Yeowell HN, Walker LC, Murad S, Pinnell SR. A common duplication in the lysyl hydroxylase gene of patients with Ehlers Danlos syndrome type VI results in preferential stimulation of lysyl hydroxylase activity and mRNA by hydralazine. Arch Biochem Biophys 1997;347:126-31.
36. van der Slot AJ, Zuurmond AM, Bardoel AF, Wijmenga C, Pruijs HE, Sillence DO, et al. Identification of PLOD2 as telopeptide lysyl hydroxylase, an important enzyme in fibrosis. J Biol Chem 2003;278:40967-72.
37. Takaluoma K, Lantto J, Myllyharju J. Lysyl hydroxylase 2 is a specific telopeptide hydroxylase, while all three isoenzymes hydroxylate collagenous sequences. Matrix Biol 2007;26:396-403.
38. Robins SP. Biochemistry and functional significance of collagen cross-linking. Biochem Soc Trans 2007;35:849-52.
39. Brinckmann J, Acil Y, Tronnier M, Notbohm H, Batge B, Schmeller W, et al. Altered x-ray diffraction pattern is accompanied by a change in the mode of cross-link formation in lipodermatosclerosis. J Invest Dermatol 1996;107:589-92.
40. van der Slot AJ, Zuurmond AM, van den Bogaerdt AJ, Ulrich MM, Middelkoop E, Boers W, et al. Increased formation of pyridinoline cross-links due to higher telopeptide lysyl hydroxylase levels is a general fibrotic phenomenon. Matrix Biol 2004;23:251-7.
41. Wu J, Reinhardt DP, Batmunkh C, Lindenmaier W, Far RK, Notbohm H, et al. Functional diversity of lysyl hydroxylase 2 in collagen synthesis of human dermal fibroblasts. Exp Cell Res 2006;312:3485-94.
42. Takaluoma K, Hyry M, Lantto J, Sormunen R, Bank RA, Kivirikko KI, et al. Tissue-specific changes in the hydroxylysine content and cross-links of collagens and alterations in fibril morphology in lysyl hydroxylase 1 knock-out mice. J Biol Chem 2007;282:6588-96.
43. Steinmann B, Eyre DR, Shao P. Urinary pyridinoline cross-links in Ehlers-Danlos syndrome type VI. Am J Hum Genet 1995;57:1505-8.
44. Schito L, Rey S, Tafani M, Zhang H, Wong CC, Russo A, et al. Hypoxia-inducible factor 1-dependent expression of platelet-derived growth factor B promotes lymphatic metastasis of hypoxic breast cancer cells. Proc Natl Acad Sci U S A 2012;109:E2707-16.
45. Wong CC, Zhang H, Gilkes DM, Chen J, Wei H, Chaturvedi P, et al. Inhibitors of hypoxia-inducible factor 1 block breast cancer metastatic niche formation and lung metastasis. J Mol Med (Berl) 2012;90:803-15.
46. Erler JT, Bennewith KL, Nicolau M, Dornhofer N, Kong C, Le QT, et al. Lysyl oxidase is essential for hypoxia-induced metastasis. Nature 2006;440:1222-6.

47. Erler JT, Bennewith KL, Cox TR, Lang G, Bird D, Koong A, et al. Hypoxia-induced lysyl oxidase is a critical mediator of bone marrow cell recruitment to form the premetastatic niche. Cancer Cell 2009;15:35-44.
48. Cailleau R, Olive M, Cruciger QV. Long-term human breast carcinoma cell lines of metastatic origin: preliminary characterization. In Vitro 1978;14:911-5.
49. Chambers AF. MDA-MB-435 and M14 cell lines: identical but not M14 melanoma? Cancer Res 2009;69:5292-3.
50. Feldser D, Agani F, Iyer NV, Pak B, Ferreira G, Semenza GL. Reciprocal positive regulation of hypoxia-inducible factor 1α and insulin-like growth factor 2. Cancer Res 1999;59:3915-8.
51. Berg RA. Determination of 3- and 4-hydroxyproline. Methods Enzymol 1982;82 Pt A:372-98.
52. Richardson AL, Wang ZC, De Nicolo A, Lu X, Brown M, Miron A, et al. X chromosomal abnormalities in basal-like human breast cancer. Cancer Cell 2006;9:121-32.
53. Rhodes DR, Yu J, Shanker K, Deshpande N, Varambally R, Ghosh D, et al. ONCOMINE: a cancer microarray database and integrated data-mining platform. Neoplasia 2004;6:1-6.
54. Comprehensive molecular portraits of human breast tumours. Nature 2012;490:61-70.
55. Pawitan Y, Bjohle J, Amler L, Borg AL, Egyhazi S, Hall P, et al. Gene expression profiling spares early breast cancer patients from adjuvant therapy: derived and validated in two population-based cohorts. Breast Cancer Res 2005;7:R953-64.
56. Hofbauer KH, Gess B, Lohaus C, Meyer HE, Katschinski D, Kurtz A. Oxygen tension regulates the expression of a group of procollagen hydroxylases. Eur J Biochem 2003;270:4515-22.
57. Zhang H, Qian DZ, Tan YS, Lee K, Gao P, Ren YR, et al. Digoxin and other cardiac glycosides inhibit HIF-1α synthesis and block tumor growth. Proc Natl Acad Sci U S A 2008;105:19579-86.
58. Reddy GK, Enwemeka CS. A simplified method for the analysis of hydroxyproline in biological tissues. Clin Biochem 1996;29:225-9.
59. Hynes RO. The extracellular matrix: not just pretty fibrils. Science 2009;326:1216-9.
60. Dong S, Nutt CL, Betensky RA, Stemmer-Rachamimov AO, Denko NC, Ligon KL, et al. Histology-based expression profiling yields novel prognostic markers in human glioblastoma. J Neuropathol Exp Neurol 2005;64:948-55.
61. Rajkumar T, Sabitha K, Vijayalakshmi N, Shirley S, Bose MV, Gopal G, et al. Identification and validation of genes involved in cervical tumourigenesis. BMC Cancer 2011;11:80.
62. Arao T, Yanagihara K, Takigahira M, Takeda M, Koizumi F, Shiratori Y, et al. ZD6474 inhibits tumor growth and intraperitoneal dissemination in a highly metastatic orthotopic gastric cancer model. Int J Cancer 2006;118:483-9.
63. Noda T, Yamamoto H, Takemasa I, Yamada D, Uemura M, Wada H, et al. PLOD2 induced under hypoxia is a novel prognostic factor for hepatocellular carcinoma after curative resection. Liver Int 2012;32:110-8.

64. Bos PD, Zhang XH, Nadal C, Shu W, Gomis RR, Nguyen DX, et al. Genes that mediate breast cancer metastasis to the brain. Nature 2009;459:1005-9.

Figure Legends

Figure 1. Knockdown of HIF-1α expression blocks PLOD1 and PLOD2 induction under hypoxic conditions. A, levels of PLOD1 and PLOD2 mRNAs were analyzed by RT-qPCR in MDA-MB-231 subclones, which were stably transfected with empty vector (shEV) or vector encoding HIF-1α shRNA (sh1α), HIF-2α shRNA (sh2α), or HIF-1α + HIF-2α shRNAs (sh1/2α), and exposed to 20% or 1% O_2 for 24 hours (mean ± SEM, $n = 3$); ***$P < 0.001$, **$P < 0.01$ versus shEV at 20% O_2; $^{###}P < 0.001$, $^{##}P < 0.05$ vs shEV at 1% O_2 (one-way ANOVA with Bonferroni post-test). B, immunoblot assays were performed using lysates prepared from MDA-MB-231 subclones exposed to 20% or 1% O_2 for 48 hours. C, immunoblot assays were performed using lysates of parental MDA-MB-231 cells that were exposed to 1% O_2 for the indicated time in hours. D, PLOD1 and PLOD2 mRNA levels were analyzed by RT-qPCR in MDA-MB-231 cells exposed to vehicle (DMSO) or 200 nM Digoxin at 20% or 1% O_2 for 24 hours. ***$P < 0.001$ vs DMSO-treated 20% O_2; $^{###}P < 0.001$ vs DMSO-treated 1% O_2 (one-way ANOVA with Bonferroni post-test).

Figure 2. PLOD1 and PLOD2 expression in breast cancer patients. A-B, *PLOD1* and *PLOD2* gene expression levels (presented as normalized microarray intensity values) in normal breast ($n = 7$) and breast cancer ($n = 40$) tissues (A) or in paired adjacent normal and breast cancer tissues from The Cancer Genome Atlas ($n = 28$) (B) are shown. The box represents the 25th through 75th percentiles and whiskers represent the minimum and maximum range of the data. *P* values were determined by Student's *t* test. C, Kaplan-Meier analysis of disease-specific survival of 159

breast cancer patients stratified by PLOD1 (left) or PLOD2 (right) mRNA expression above the median level (High) or below the median level (Low).

Figure 3. PLOD2 knockdown in MDA-MB-231 cells inhibits local tissue invasion. A, immunoblot assays were performed using lysates prepared from MDA-MB-231 control (shLKO.1) or PLOD2-knockdown (shPL2-1 and shPL2-2) subclones exposed to 20% or 1% O_2 for 48 hours. B, proliferation of subclones was determined by trypan blue staining on the indicated days. Crystal violet staining of tissue culture dishes on day 12 is shown (right). C-E, the subclones were injected into the MFP of NOD-SCID mice and tumor volume was plotted versus time (C), final tumor weight (in grams) was determined (D), and human PLOD2 mRNA levels were determined by RT-qPCR (E; mean ± SEM, $n = 5$, one-way ANOVA with Bonferroni post-test; $^{***}P < 0.001$, $^{**}P < 0.01$ versus shLKO.1). F, immunohistochemical staining of primary tumor sections for PLOD2 is shown. Scale bar = 500 μm. G, immunohistochemical staining of primary tumor sections for HIF-1α and PLOD2 is shown. Images were deconvoluted and pseudocolored to assess colocalization (right). Scale bar = 500 μm. H, hematoxylin staining of primary tumor sections. Invasion of shLKO.1 into adipose tissue (red arrow) or muscle (black arrow) is shown in the upper panel. The boundary between shPL2 cells and normal tissue is indicated by dashed line in the lower panel. Scale bar = 500 μm.

Figure 4. PLOD2 is essential for lymph node and lung metastasis. A, human genomic DNA content in lungs of tumor-bearing mice was quantified using qPCR with human-specific *HK2* gene primers (mean ± SEM, $n = 5$, one-way ANOVA). B, lung sections (5 x 5 mm) were stained with hematoxylin and eosin. C, metastatic area was determined by image analysis of 5 x 5 mm

lung sections (mean ± SEM, $n = 5$, one-way ANOVA). D, the number of metastatic foci per 5 x 5 mm tumor section was determined (mean ± SEM, $n = 5$, one-way ANOVA). E, axillary lymph node sections were subjected to immunohistochemistry using an antibody specific for human vimentin. Staining of whole lymph nodes in 3.5 x 3.5 mm sections with preserved lymph node structure outlined in dashed line on left. High-power field of lymph node follicles is shown on right. Scale bar = 100 μm. F-G, vimentin staining (F) was quantified by image analysis (G; mean ± SEM, $n = 5$, one-way ANOVA). Bonferroni post-tests were performed for all ANOVAs. $^{**}P < 0.01$, $^{***}P < 0.001$ vs. shLKO.1.

Figure 5. PLOD2 expression decreases fibrillar collagen formation but not total collagen deposition. A, collagen 1A1 protein levels in conditioned media and cell lysate of MDA-MB-231 subclones exposed to 1% O_2 for 72 hours were determined by immunoblot assay. Actin was used as a loading control for cell lysate. Ponceau S staining was used as a loading control for conditioned media. B, collagen content of tumors was determined using the collagen hydroxyproline assay. C, tumor sections from the indicated subclones were stained with picrosirius red and imaged under circularly polarized light (top) and collagen fiber staining was thresholded and subjected to image analysis (bottom). D, picrosirius red staining of 3 sections from 5 mice per group was quantified by image analysis to determine the area of the tumor section occupied by collagen fibers (% fibrillar collagen; mean ± SEM, one-way ANOVA). E, the stiffness of freshly dissected control (shLKO.1) or shPLOD2 tumors was determined (mean ± SEM, one-way ANOVA). F, picrosirius red staining to detect crosslinked collagen fibers (left) and immunohistochemical staining to detect PLOD2 (right) were performed on serial control

tumor sections. Bonferroni post-test was performed for all ANOVAs. *P<0.05, **P < 0.01, ***P < 0.001 vs. shLKO.1 in panels D and E.

Figure 6. PLOD2 is essential for invasion and metastasis of MDA-MB-435 cells. A, immunoblot assays were performed using lysates prepared from control (shLKO.1) or PLOD2-knockdown (shPL2-1 and shPL2-2) MDA-MB-435 subclones exposed to 20% or 1% O_2 for 48 hours. B, the indicated subclones were injected into the MFP of NOD-SCID mice and tumor volume was plotted versus time. C, hematoxylin staining of primary tumor sections. Invasion of shLKO.1 into adipose tissue (red arrow) is shown in the left panel. The well-defined boundary between shPL2 cells and normal tissue is indicated by the dashed line in the right panel. Scale bar = .5 mm. D, lung sections (5 x 5 mm) were stained with hematoxylin and eosin. E, metastatic area was determined by image analysis (mean ± SEM, n = 5, one-way ANOVA). F, the number of metastatic foci per 5 x 5 mm tumor section was determined (mean ± SEM, n = 5, one-way ANOVA). G, human genomic DNA content in mouse lungs was quantified using qPCR with human-specific *HK2* gene primers (mean ± SEM, n = 5, one-way ANOVA). H, ipsilateral axillary lymph node sections were subjected to immunohistochemistry using an antibody specific for human vimentin. Scale bar = 100 μm. I, vimentin staining was quantified by image analysis (mean ± SEM, n = 5, one-way ANOVA). J, the stiffness of freshly dissected control or shPLOD2 tumors was determined. Bonferroni post-tests were performed for all ANOVAs. *P<0.05, **P < 0.01, ***P < 0.001 vs. shLKO.1.

Figure 7. Hypoxia-induced and HIF-1-dependent expression of PLOD2 and LOX family members mediate crosslinking of collagen fibers, leading to increased invasion and metastasis of breast cancer cells.

Figure 1

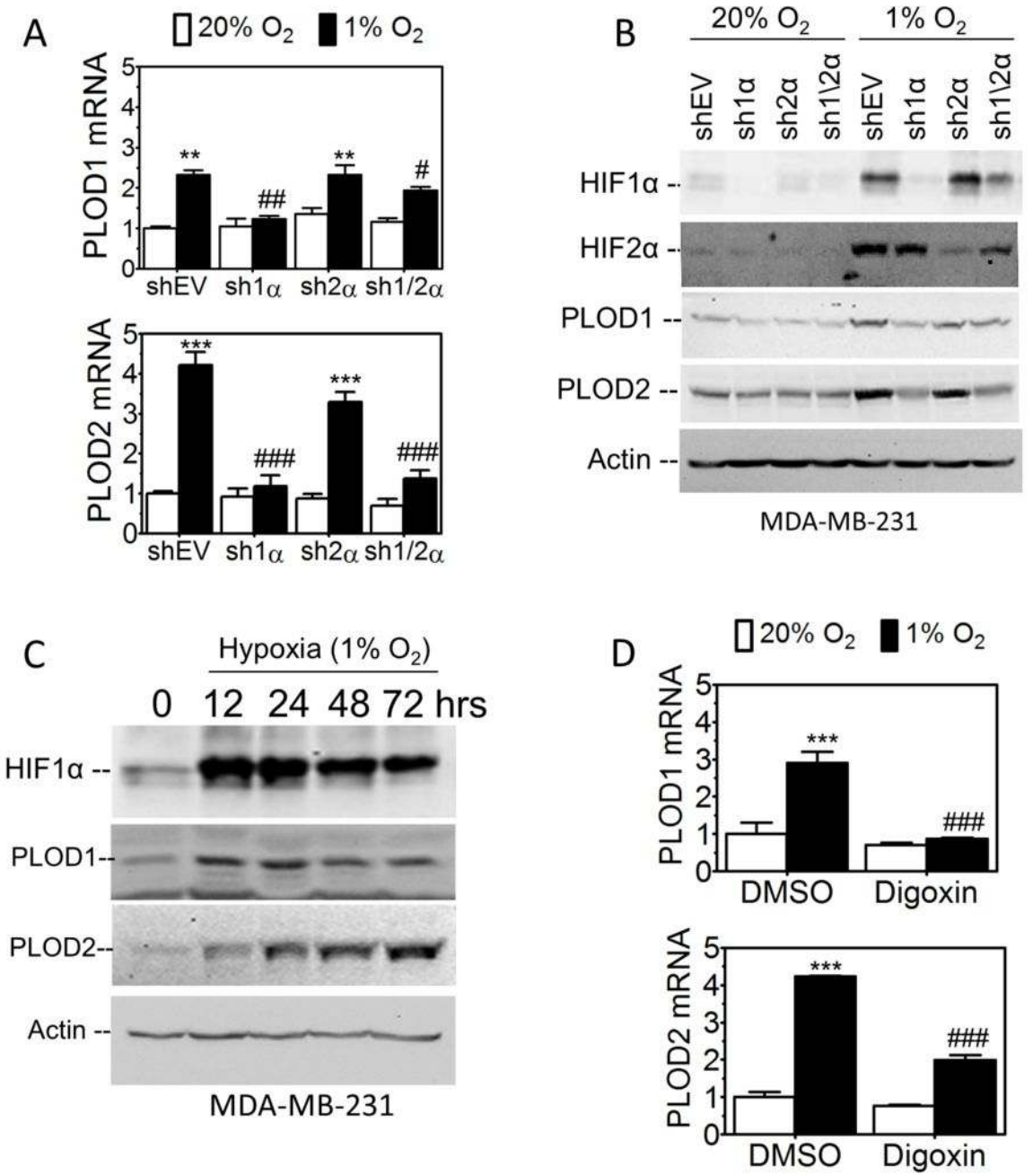

Figure 2

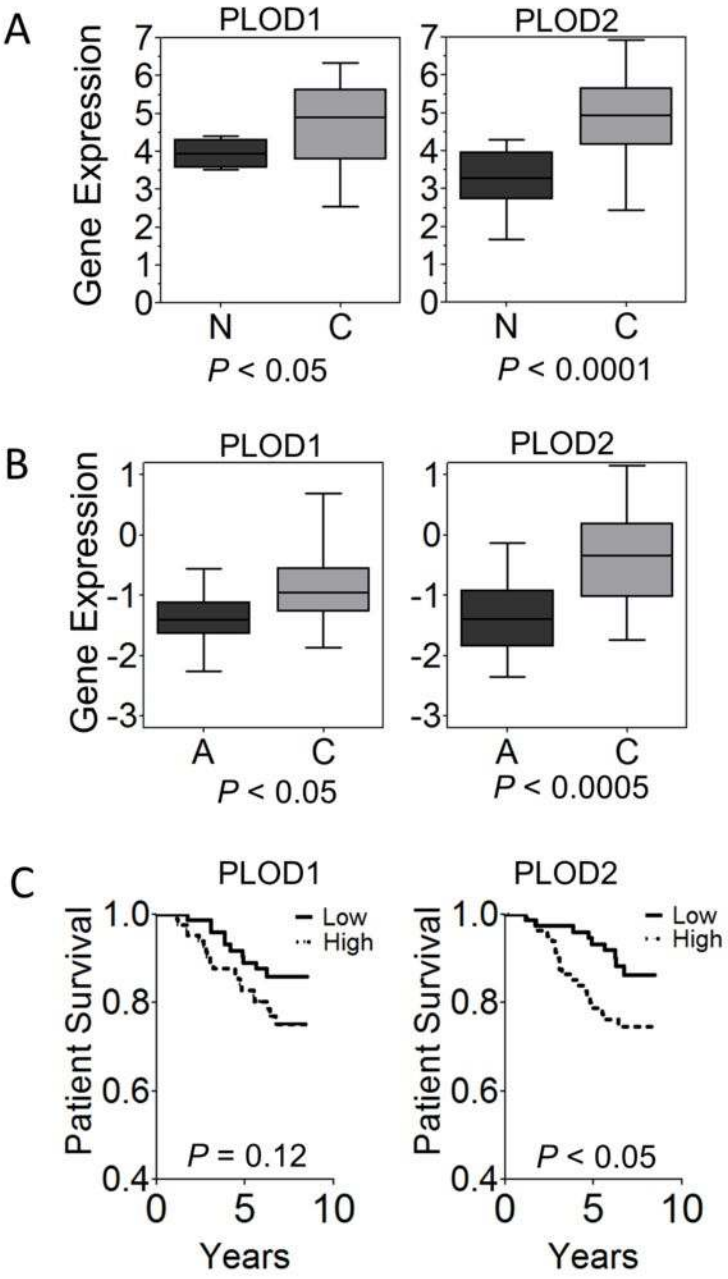

Figure 3

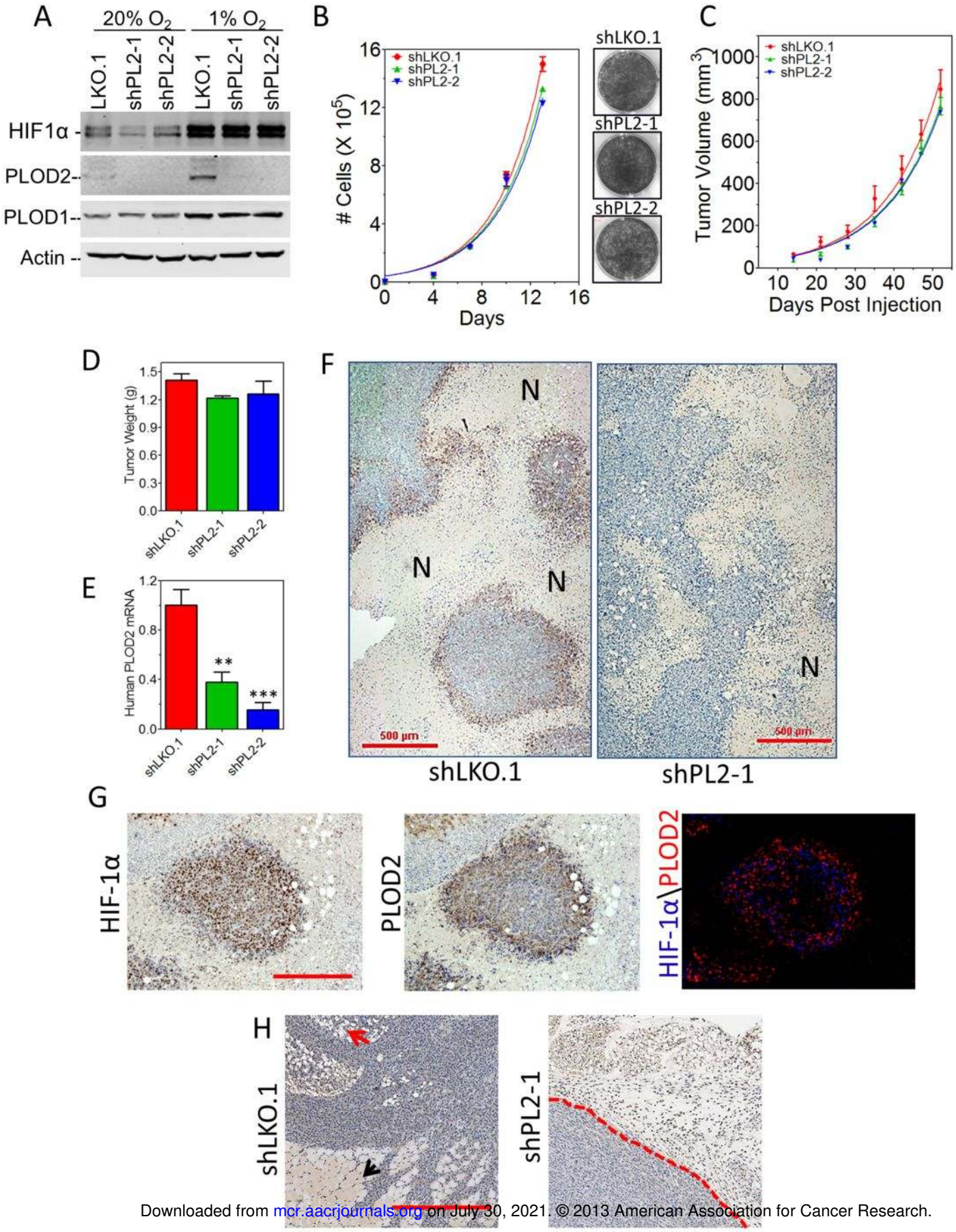

Figure 4

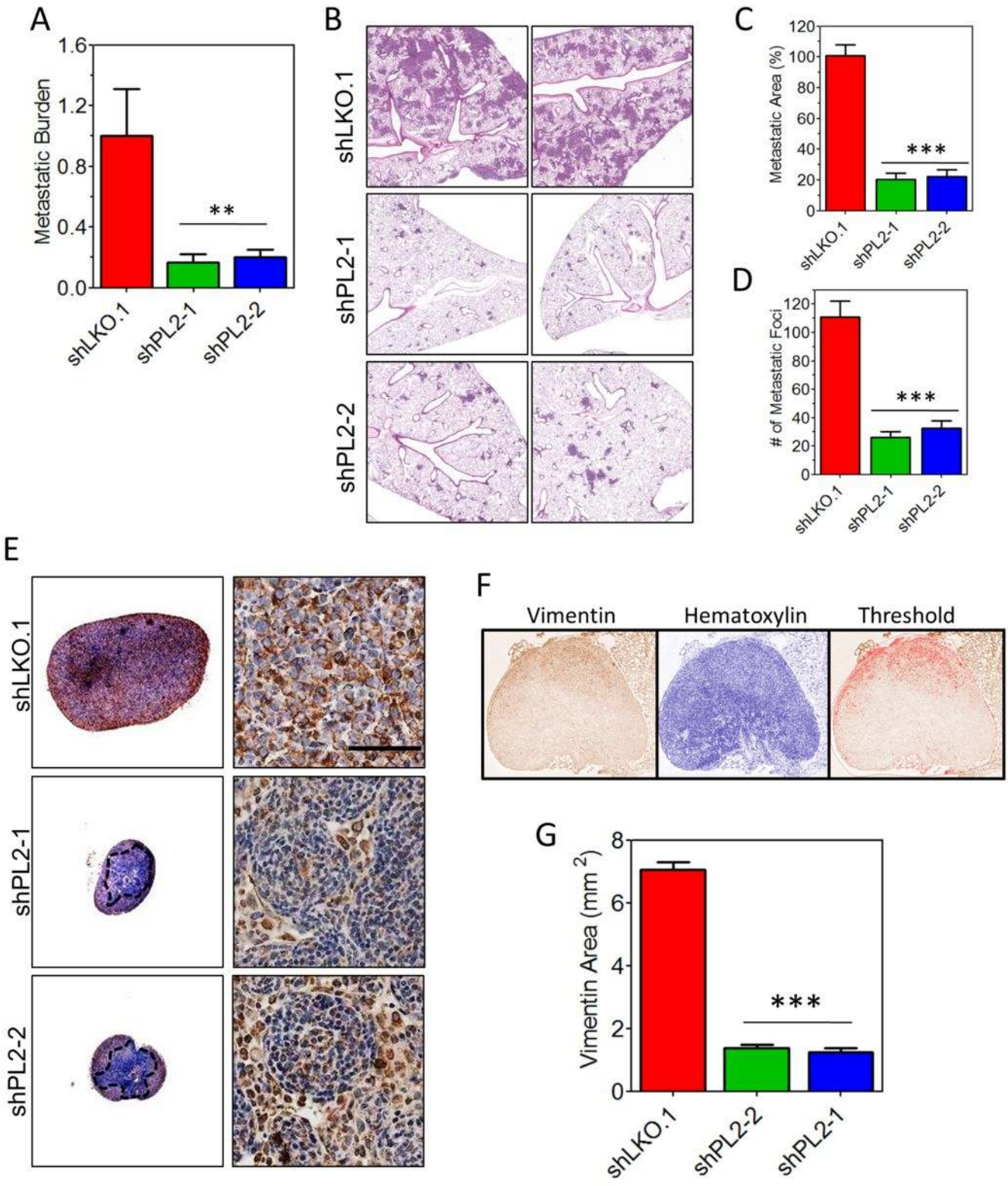

Figure 5

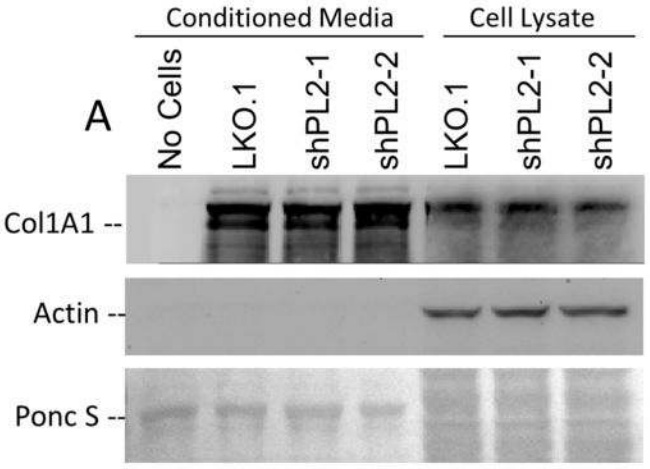

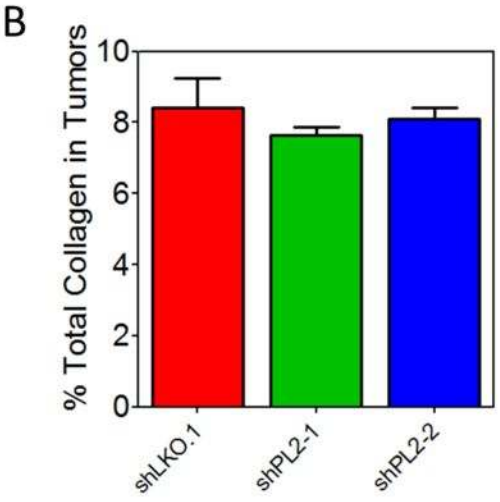

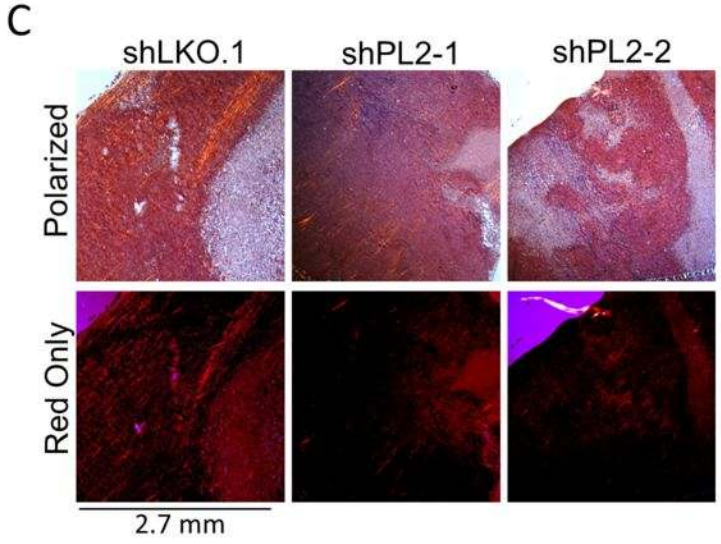

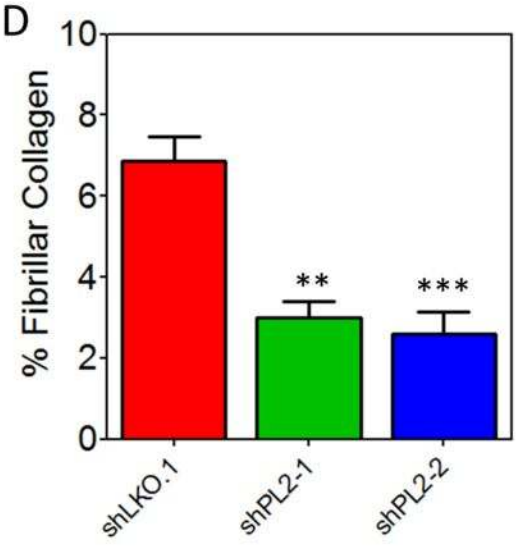

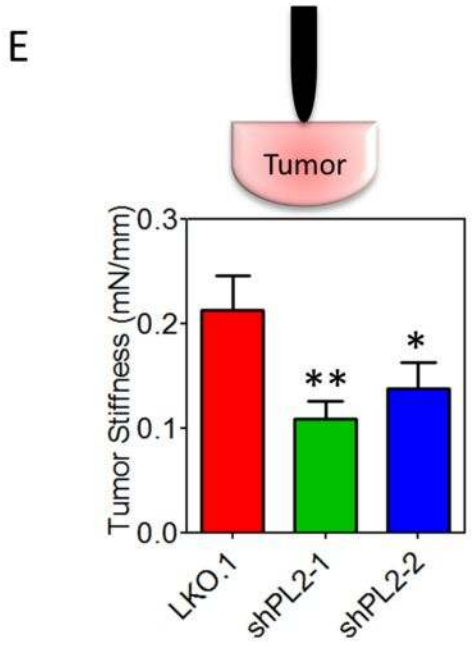

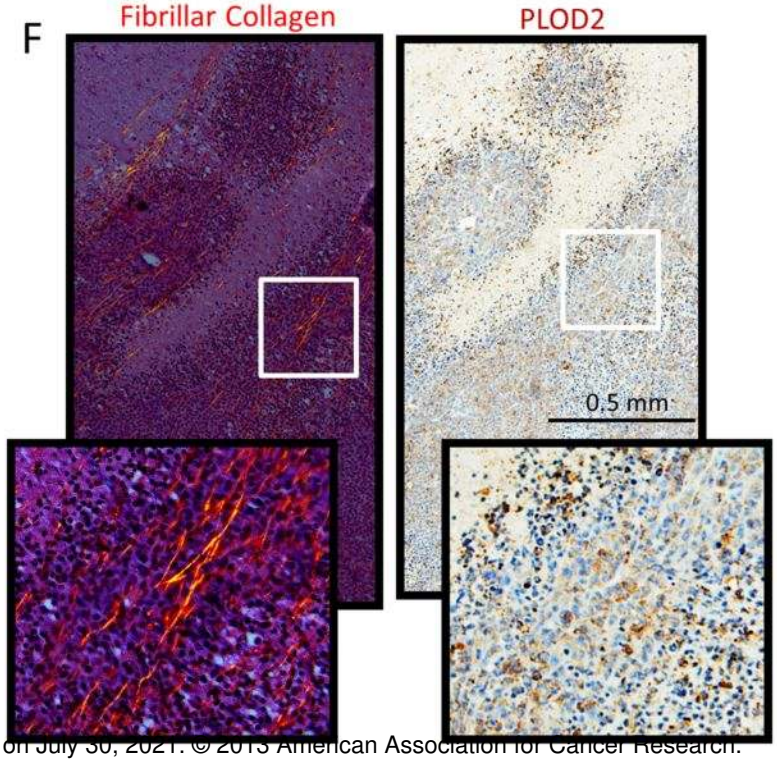

Figure 6

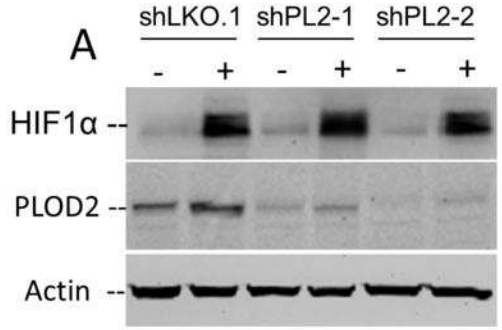

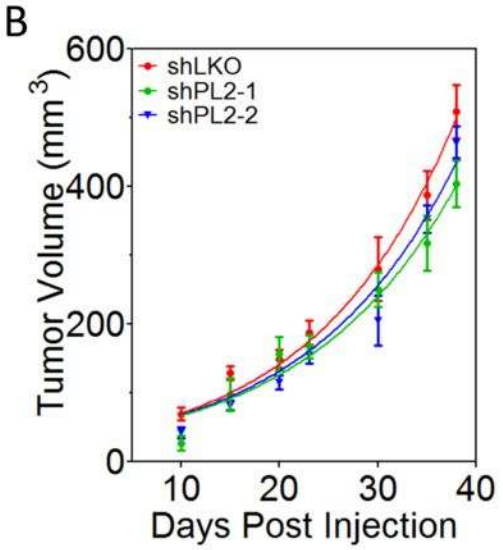

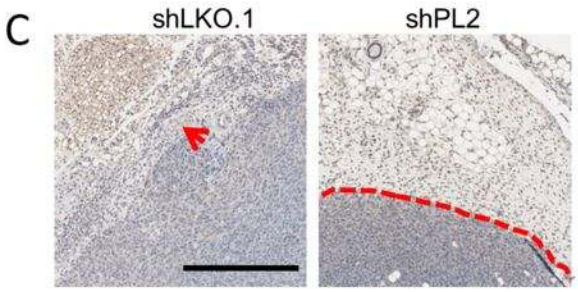

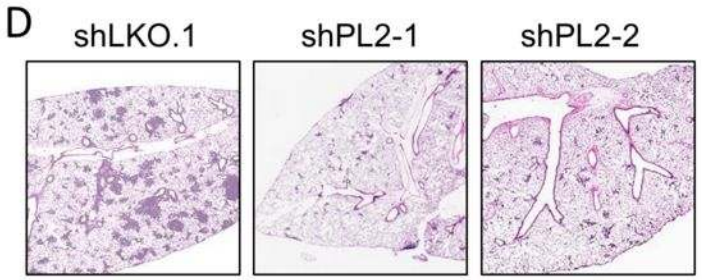

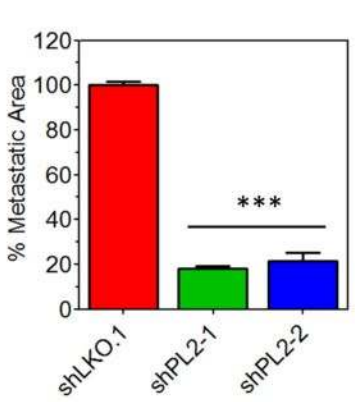

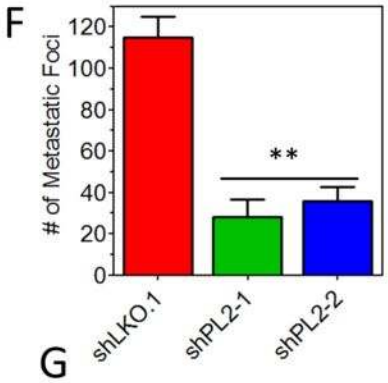

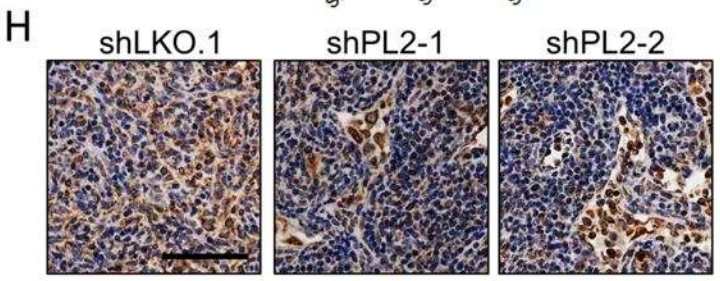

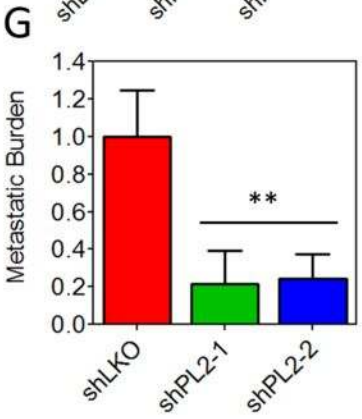

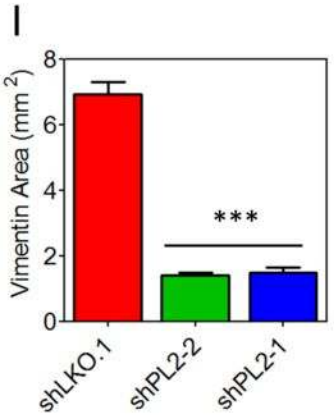

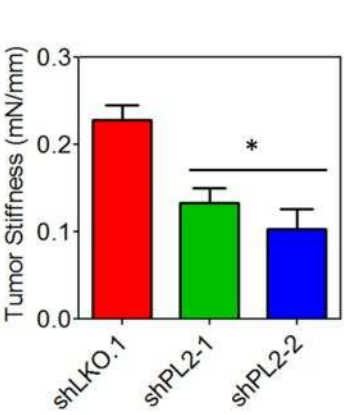

Figure 7

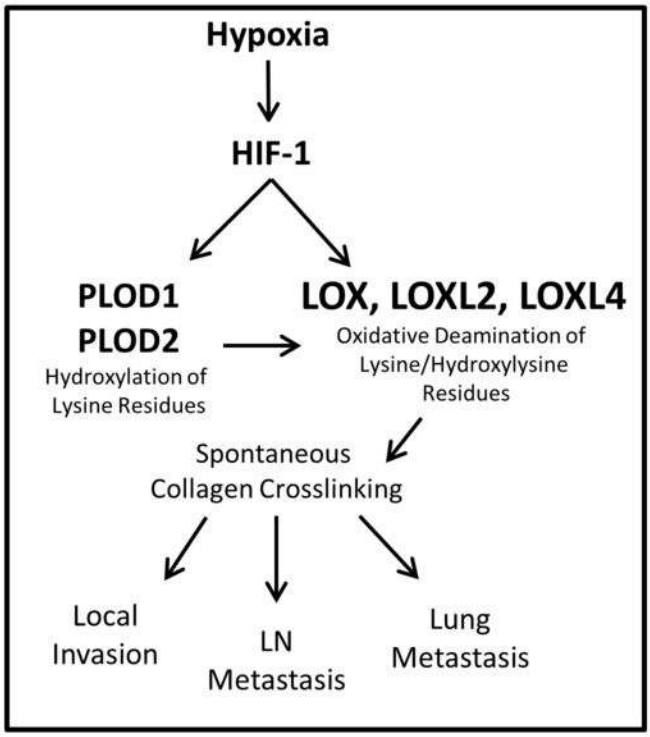

AACR American Association for Cancer Research

Molecular Cancer Research

Procollagen Lysyl Hydroxylase 2 is Essential for Breast Cancer Metastasis

Daniele Gilkes, Saumendra Bajpai, Carmen Chak-Lui Wong, et al.

Mol Cancer Res Published OnlineFirst February 1, 2013.